n, to obtain the anticipated classical-type modes for the conical shells, although very careful slow-frequency sweeps were made with all forementioned shaker configurations for each mode investigated.

The methods of Goldberg were used to compute the response of one of the authors' free-free conical shells to a concentrated, simple harmonic forcing function placed normal to the shell at the major diameter. When the forcing frequency was only 5% higher than the natural frequency of the $n = 5$ mode, the nodal patterns produced were similar to those reported in the note. A similar pattern was also produced when the forcing frequency was 20% higher than the natural frequency for $n = 5$. A point of interest in this connection is the fact that a smooth curve can be drawn through the data points which depict the frequency-n relationship for the response at the major diameter in the authors' note. This was true for all four of the frustums tested and would seem highly unlikely if the responses measured were primarily forced responses.

It is felt that certain system parameters may prove to be critical in the case of free-free conical frustum shells. Among these are conicity, modal frequency density, material and acoustic damping, length-to-thickness ratio, and radius-to-thickness ratio. Although it may be possible to design an experiment that yields the anticipated classical mode shapes, variations of these parameters which might explain the existence of nodal patterns such as obtained during this investigation should be considered. For instance, in the case of Hu's experiments the modal frequency density was about one-half that of the authors' experiment. Closer proximity of adjacent natural frequencies in combination with material or acoustic damping may result in the inherent coupling of classical type modes to give the nodal patterns the authors obtained.

References

[1] Herr, R. W., "A wide-frequency-range air jet shaker," NACA TN 4060 (1957).

[2] Goldberg, J. E., Bogdanoff, J. L., and Alspaugh, D. W., "On the calculation of the modes and frequencies of vibration of pressurized conical shells," *AIAA 5th Annual Structural and Materials Conference* (AIAA, New York, 1964), pp. 243–249.

[3] Mixson, J. S. and Herr, R. W., "An investigation of the vibration characteristics of pressurized thin-walled circular cylinders partly filled with liquid," NASA TR R-145 (1962).

Comments on "Laminar Flow in Plane Wakes of a Conducting Fluid in the Presence of a Transverse Magnetic Field"

Lit S. Han*
Ohio State University, Columbus, Ohio

In a recent note by Gupta[1], the familiar wake equation is analyzed with respect to asymptotic solutions for large x, the latter being the distance behind the trailing edge of an obstacle. Using the notations of the referenced note, the equation is

$$Uu_x = \nu u_{yy} - (\sigma\mu^2 H_0^2/\rho)u \tag{1}$$

where u is the velocity defect, σ is the electrical conductivity, and H_0 is the applied transverse magnetic field not necessarily a constant. The boundary conditions are $u(x, \infty) = 0$ and $u_y(x, 0) = 0$.

Received September 30, 1964.
* Professor of Mechanical Engineering.

Since the equation is linear one may attempt a solution of the form

$$u = f(x)F(x, y) \tag{2}$$

where the property of self-similarity is embedded in F. Inserting (2) into (1) yields

$$U[f'F + fF_x] = \nu fF_{yy} - (\sigma\mu^2 H_0^2/\rho)fF \tag{3}$$

Whence decoupling of the functions produces

$$f = \exp[- \int_{x_0}^{x} \frac{\sigma\mu^2 H_0^2}{\rho} \frac{1}{U} dx] \tag{4}$$

and

$$UF_x = \nu F_{yy} \tag{5}$$

The solution of (5) using the notations in the note becomes

$$F = \sum_{n=0}^{\infty} A_n \frac{x}{x_0}^{-n-(1/2)} g_n(\xi) \tag{6}$$

The magnetic modification factor is expressed by (4), which shows $f \approx (x/x_0)^{-c}$ if $H_0 \sim x^{-1/2}$ and $f \sim \exp(-bx)$ if H_0 is a constant so that in the latter case similarity is still preserved in direct contradistinction with the contention in the reference.

Reference

[1] Gupta, A. S., "Laminar flow is plane wakes of a conducting fluid in the presence of a transverse magnetic field," AIAA J. 1, 2391–2392 (1963).

Reply by Author to L. S. Han

A. S. Gupta*
Indian Institute of Technology, Kharagpur, India

The author wishes to thank Han for pointing out the possibility of another similarity solution of the wake equation [Eq. (4) of my note] for the case of a uniform magnetic field in the form

$$u = \exp(-bx)\cdot F(x, y) \tag{1}$$

where F satisfies

$$UF_x = \nu F_{yy} \tag{2}$$

This solution that is derived by Han in a slightly different way can also be obtained from the set of Eqs. (7) of my note if, instead of taking $UCC'/\nu = 2$, we equate UCC'/ν to zero, in which case $C(x)$ reduces to a nonzero constant. [$C = 0$ being impossible by virtue of the Eq. (5) of my note.] In this case the second equation of the set (7) leads to $a(x) \sim \exp(-bx)$, and the third equation becomes valid for a uniform magnetic field.

Unfortunately, however, the preceding Eq. (2) does not admit of a solution satisfying the boundary conditions $F(x, \infty) = 0$ [corresponding to $u(x, \infty) = 0$] and $F_y(x, 0) = 0$ [corresponding to $u_y(x, 0) = 0$]. This can be seen in the following way.

Let the solution of the foregoing Eq. (2) be taken in the form

$$F = F(\eta) \qquad \eta = yD(x) \tag{3}$$

so that Eq. (2) becomes

$$\eta F'(\eta) \times D'(x)/D(x) = \nu F''(\eta)/U \times D^2 \tag{4}$$

Received October 26, 1964.
* Assistant Professor of Mathematics.

Hence for a similarity solution either $D' = 0$ or $D'(x)/D(x) = \alpha D^2, \alpha \neq 0$. In the former case $\eta = \text{const}\, y$. Equation (4) then gives $F''(\eta) = 0$, and its solution $F = A + B\eta$ clearly fails to satisfy $F(\infty) = F'(0) = 0$ unless $A = B = 0$, in which case, $F(\eta) \equiv 0$. In the latter case $D(x) \sim x^{-1/2}$ so that $\eta \sim yx^{-1/2}$. Now taking $\eta = yU^{1/2}/2(\nu x)^{1/2}$, Eq. (2) becomes

$$F'' + 2\eta F' = 0$$

which on integration gives $F'(\eta) = A_1 e^{-\eta^2}$. Since $F'(0) = 0$, $F'(\eta) \equiv 0$, and its solution satisfying $F(\infty) = 0$ is clearly $F(\eta) \equiv 0$. Thus there is no nontrivial similarity solution of Eq. (2) satisfying $F(\infty) = F'(0) = 0$.

The same conclusion can be reached from Eq. (6) of my note. When $UCC'/\nu = 0$, Eq. (6) can be put in the form

$$f'' + \lambda_1 f = 0 \tag{5}$$

λ_1 being a constant, and Eq. (5) clearly has no nontrivial solution satisfying $f(\infty) = 0$; $f'(0) = 0$ for all the three cases $\lambda_1 > 0$, $\lambda_1 = 0$, and $\lambda_1 < 0$.

Comment on "Basis for Derivation of Matrices for the Direct Stiffness Method"

J. L. Tocher*
The Boeing Co., Renton, Wash.

AND

K. K. Kapur†
University of Washington, Seattle, Wash.

In a recent article, Melosh[1] presents a stiffness matrix for a rectangular plate element that may be used for plate bending analysis. There are several errors in the stiffness matrix that should be corrected. Also the matrix can be presented in a more compact form by noting that the stiffness coefficients for nodes 2, 3, and 4 of the plate can be obtained by proper permutations and sign changes of the stiffness coefficients for node 1. These relations are given by the stiffness matrix in Fig. 1. The coefficients describing the behavior of node 1 (the first three columns of the stiffness matrix) are given in Fig. 2. It should be noted that for an isotropic plate, the coefficients in the moment-curvature relationship have the following values:

$$A_{11} = A_{22} = D$$

$$A_{21} = A_{12} = \nu D$$

$$A_{33} = (1 - \nu)D$$

$$\begin{pmatrix} Z_1 \\ M_{x1}/a \\ M_{y1}/b \\ Z_2 \\ M_{x2}/a \\ M_{y2}/b \\ Z_3 \\ M_{x3}/a \\ M_{y3}/b \\ Z_4 \\ M_{x4}/a \\ M_{y4}/b \end{pmatrix} = \begin{pmatrix} K_{11} & & & & & & & & & & & \\ K_{21} & K_{22} & & & & & & & & & & \\ K_{31} & K_{32} & K_{33} & & & & & \text{SYMMETRIC} & & & & \\ K_{41} & K_{42} & K_{43} & K_{11} & & & & & & & & \\ K_{51} & K_{52} & K_{53} & K_{21} & K_{22} & & & & & & & \\ K_{61} & K_{62} & K_{63} & -K_{31} & -K_{32} & K_{33} & & & & & & \\ K_{71} & K_{72} & K_{73} & K_{10,1} & K_{10,2} & -K_{10,3} & K_{11} & & & & & \\ K_{81} & K_{82} & K_{83} & K_{11,1} & K_{11,2} & -K_{11,3} & -K_{21} & K_{22} & & & & \\ K_{91} & K_{92} & K_{93} & -K_{12,1} & -K_{12,2} & K_{12,3} & -K_{31} & K_{32} & K_{33} & & & \\ K_{10,1} & K_{10,2} & K_{10,3} & K_{71} & K_{72} & -K_{73} & K_{41} & -K_{42} & -K_{43} & K_{11} & & \\ K_{11,1} & K_{11,2} & K_{11,3} & K_{81} & K_{82} & -K_{83} & -K_{51} & K_{52} & K_{53} & -K_{21} & K_{22} & \\ K_{12,1} & K_{12,2} & K_{12,3} & -K_{91} & -K_{92} & K_{93} & -K_{61} & K_{62} & K_{63} & K_{31} & -K_{32} & K_{33} \end{pmatrix} \cdot \begin{pmatrix} w_1 \\ a\,w_{1,x} \\ b\,w_{1,y} \\ w_2 \\ a\,w_{2,x} \\ b\,w_{2,y} \\ w_3 \\ a\,w_{3,x} \\ b\,w_{3,y} \\ w_4 \\ a\,w_{4,x} \\ b\,w_{4,y} \end{pmatrix}$$

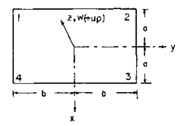

Fig. 1 Basic stiffness coefficient relationships.

$$\begin{pmatrix} K_{11} & & \\ K_{21} & K_{22} & \\ K_{31} & K_{32} & K_{33} \\ K_{41} & K_{42} & K_{43} \\ K_{51} & K_{52} & K_{53} \\ K_{61} & K_{62} & K_{63} \\ K_{71} & K_{72} & K_{73} \\ K_{81} & K_{82} & K_{83} \\ K_{91} & K_{92} & K_{93} \\ K_{10,1} & K_{10,2} & K_{10,3} \\ K_{11,1} & K_{11,2} & K_{11,3} \\ K_{12,1} & K_{12,2} & K_{12,3} \end{pmatrix} = \left(\frac{b}{6a^3}\right)A_{11} \begin{pmatrix} 6 & & \\ 6 & 8 & \\ 0 & 0 & 0 \\ 3 & 3 & 0 \\ 3 & 4 & 0 \\ 0 & 0 & 0 \\ -3 & -3 & 0 \\ 3 & 2 & 0 \\ 0 & 0 & 0 \\ -6 & -6 & 0 \\ 6 & 4 & 0 \\ 0 & 0 & 0 \end{pmatrix} + \left(\frac{a}{6b^3}\right)A_{22} \begin{pmatrix} 6 & & \\ 0 & 0 & \\ 6 & 0 & 8 \\ -6 & 0 & -6 \\ 0 & 0 & 0 \\ 6 & 0 & 4 \\ -3 & 0 & -3 \\ 0 & 0 & 0 \\ 3 & 0 & 2 \\ 3 & 0 & 3 \\ 0 & 0 & 0 \\ 3 & 0 & 4 \end{pmatrix} + \left(\frac{1}{2ab}\right)A_{21} \begin{pmatrix} 1 & & \\ 1 & 0 & \\ 1 & 2 & 0 \\ -1 & -1 & 0 \\ -1 & 0 & 0 \\ 0 & 0 & 0 \\ 1 & 0 & 0 \\ 0 & 0 & 0 \\ 0 & 0 & 0 \\ -1 & 0 & -1 \\ 0 & 0 & 0 \\ -1 & 0 & 0 \end{pmatrix} + \left(\frac{1}{30ab}\right)A_{33} \begin{pmatrix} 21 & & \\ 3 & 8 & \\ 3 & 0 & 8 \\ -21 & -3 & -3 \\ -3 & -8 & 0 \\ 3 & 0 & -2 \\ 21 & 3 & 3 \\ -3 & 2 & 0 \\ -3 & 0 & 2 \\ -21 & -3 & -3 \\ 3 & -2 & 0 \\ -3 & 0 & -8 \end{pmatrix}$$

Fig. 2 Stiffness coefficients for node 1.

where D represents the flexural rigidity of the plate,

$$D = Et^3/12(1 - \nu^2)$$

Numerical convergence studies of this stiffness matrix have indicated that it performs adequately, although the monotonic behavior predicted by Melosh does not always occur. Table 1 gives numerical factors for the maximum deflection of a square plate that illustrate convergence behavior of this element. The clamped plate with a central concentrated load does not behave monotonically for a very coarse "mesh." This lack of monotonicity is probably because the four-element approximation of the clamped plate cannot differentiate between a central concentrated load and a uniformly distributed load. In both cases there is only one equation in one unknown to be solved.

It also should be noted that convergence may occur from "above" as well as from "below." This is due to lack of slope continuity along adjacent edges of the plate elements, as was pointed out by Pian.[2] If the element edges were continuous with respect to displacements and slopes (not just displacements), then the elements would always be stiffer than the actual plate and convergence would always be from "below."

Table 1 Computed central deflection of a square plate for several "meshes"[a]

Mesh size	Total no. of nodes	Simply supported plate		Clamped plate	
		α (Uniform load)	β (Concentrated load)	α (Uniform load)	β (Concentrated load)
(2×2)	9	0.003446	0.013784	0.001480	0.005919
(4×4)	25	0.003939	0.012327	0.001403	0.006134
(8×8)	81	0.004033	0.011829	0.001304	0.005803
(12×12)	169	0.004050	0.011715	0.001283	0.005710
(16×16)	289	0.004056	0.011671	0.001275	0.005672
Exact (Timoshenko)		0.004062	0.01160	0.00126	0.00560

[a] $w_{max} = \alpha q a^4/D$ for a uniformly distributed load q; $w_{max} = \beta P a^2/D$ for a central concentrated load P.

Received December 21, 1964.

* Research Engineer, Mathematical Analysis Unit, Airplane Division.

† Graduate Student.